Laser Frequency Stabilization Using Saturated Absorption of the 6573 Å Line of Calcium

R. L. Barger, J. B. West* and T. C. English†

Until recently, the search for ultrastable wavelength/frequency standards in the visible spectrum has been limited to the very narrow regions corresponding to the Doppler gain widths of gas lasers. Few coincidences have been found, two of which are those of the He-Ne laser with I_2 at 6328 Å and the Ar^+ laser with I_2 at 5145 Å. These result in good intermediate accuracy standards. The development of fast stabilization of tunable cw dye lasers[1] now makes it possible to use any suitable, long-lived transition anywhere in the visible region. Thus, one can investigate saturated absorption transitions such as the $^1S_o - {}^3P_1$ in Ca and Mg,[2,3] or suitable two-photon transitions such as the $^2S_{\frac{1}{2}} - {}^2D_{5/2}$ in Ag and the $^4S_{3/2} - {}^2P_{3/2}$ in Bi.[4] In this paper we describe our investigations of the calcium intercombination $^1S_o - {}^3P_1$ line at 6573 Å in both an absorption cell and an atomic beam.

The properties of this transition are given in Table I. The narrow lifetime-limited linewidth of 410 Hz, the low Stark and Zeeman shifts, absence of intensity shifts (the recoil doublet splitting of 23 kHz can be fully resolved), and the possibility to measure the second-order Doppler shift with atomic beam techniques as described below make this transition in calcium a prime candidate for an ultra-high accuracy wavelength/frequency standard in the visible.

* Present address: Northrup Laser Labs, 3401 W. Broadway, Hawthorne, CA 90250

† Present address: Efratom California, INc., 3303 Harbor Blvd, Costa Mesa, CA.

Fast-Stabilized cw Dye Laser

The stabilized cw dye laser used in this work is described in detail elsewhere,[1] so only a brief discussion will be given here. The stabilization scheme is indicated in Fig. 1. The dye laser frequency is locked to a transmission fringe of the servo cavity. The servo signal is split into slow and fast parts with the crossover at 1 kHz. The slow correction is applied to the output mirror PZT, and the fast correction to an intracavity AD*P phase modulator crystal. The unity gain point of the servo is at 0.3 μsec. This frequency lock results in the frequency stability shown by curve B in the Allan variance plot of Fig. 2. The short term jitter of about 1 kHz indicates that line widths as narrow as 1 kHz could be observed with the laser.

The deterioration of the stability beyond about ½ sec, as seen in curve B, is caused by long term temperature drifts of the servo cavity which is not thermally isolated. These drifts are eliminated by locking the servo cavity length to a fringe of a CH_4-stabilized 3.39 μm He-Ne laser through a 3.39 μm frequency-offset-locked local oscillator, as indicated in Fig. 1. The unity gain point for the servo cavity lock is at about 0.1 sec. The resulting dramatic improvement in long term stability is seen in curve A of Fig. 2. The stability is still improving at an integration time of 300 sec, where it has a value of 6×10^{-13}. It should flicker out at a level of about 1×10^{-13}, this level being determined by the stability of the particular CH_4-stabilized laser which was used. To stabilize the dye laser frequency to the Ca line, the servo cavity length lock can be switched from the 3.39 μm fringe signal to the Ca line signal from the atomic beam. Then the dye laser long-term frequency stability will be determined by the properties of the Ca line.

The dye laser intensity is stabilized[5] with an AD*P polarization rotator and linear polarizer not shown in Fig. 1. These are located in the dye laser output beam. The intensity transmitted by the polarizer is detected and amplifed with a fast amplifier (similar to that used in the frequency servo); the resulting signal is applied to the AD*P crystal to close the servo loop. This technique improves the intensity stability from its free-running level of several percent to a nearly constant level of about 1×10^{-4} for integration times between 10^{-4} and 10 sec.

Ca Absorption Cell

A fairly sharp saturated absorption line is easily obtained with an absorption cell external to the laser cavity. The absorption coefficient is large (from our measurements we obtain a coefficient of about .03 cm^{-1} $Pascal^{-1}$ (4 cm^{-1} $Torr^{-1}$); thus a cell of convenient size can be used.

The cell set-up is indicated in Fig. 3. The quartz tube is 40 cm long, 15 mm in diam., and has quartz end windows. The middle 20 cm of the tube is contained in an oven to bring the calcium temperature up to about 600^{o} C. This temperature produces a calcium vapor pressure of about 1.3 Pascal (10 m Torr). The portion of the cell within the oven was lined with a niobium tube to prevent reactions between the hot quartz and calcium vapor. A buffer gas, argon at a few tens of Pascals (a few tenths of a Torr), was used to prevent rapid migration of calcium out of the hot region. This design is similar to that reported by Furcinitti, et al.[6] Helmholtz coils were used to reduce the earths magnetic field in the absorption region. The laser beam was focussed with a 40 cm focal length lens to produce a waist diameter of about 100 μm at the center of the cell. A few percent transmitting cat's eye[7] at the output end of the cell gave a refocussed

retro-reflected beam. The light transmitted through the cat's eye was amplified and recorded with a multi-channel analyser.

Fig. 4 shows a typical saturation peak detected with 0.1 Torr of argon buffer gas and with the calcium absorbing about 30 per cent of the light. The laser power was 5 mW. The saturated absorption peak height is about 2% of the background intensity, and the linewidth (HWHM) is about 2 MHz. There is no hyperfine structure in this transition, so the peak is symmetric and centered on the Doppler absorption profile. Thus the laser frequency can be locked to line center without the systematic shifts caused by baseline tilts. The high S/N ratio readily obtainable and the symmetry of the line indicate that a frequency reproducibility better than that of the 6328 Å iodine-stabilized laser by at least an order of magnitude should be obtained with suitable frequency locking techniques.

While measuring Zeeman effects with polarization techniques, we have observed a new effect, laser-saturated Faraday rotation. This effect for Doppler width absorptions was first observed by Faraday[8] in 1846 (it is pleasant to rediscover this old physics with modern laser techniques). One of the early observations in sodium vapor is shown in Fig. 5, which is reproduced from R. W. Wood's Physical Optics[9] and demonstrates the qualitative line shape to be expected.

The experimental conditions are indicated in Fig. 3. A longitudinal magnetic field H of a few Gauss is produced by a solenoid. The input light is linearly polarized and thus can be decomposed into two ($\pm$) circularly polarized components. With this polarization, only the $\pm\sigma$ ($\Delta m = \pm 1$) Zeeman transitions are allowed. The output light is analyzed with a linear polarizer rotated an angle θ with respect to the input

polarization. Under these conditions, both saturated absorption and saturated dispersion can be detected.

As the laser frequency is tuned across the transition, the birefringence corresponding to the difference in refractive index for the $\pm\sigma$ components produces a rotation of the detected linear polarization. The signal detected through the analysing polarizer is a plot of the saturated Faraday rotation, similar in appearance to the old curves in Fig. 5 but with a line width free of Doppler broadening. The signal also contains the $\pm\sigma$ saturated absorption peaks and the Doppler-generated level crossing[10] peak.

Typical observed curves are shown in Fig. 6. The center curve is the Zeeman pattern obtained with $\theta = 0$, showing the $\pm\sigma$ and level-crossing peaks. The upper and lower curves were obtained with the magnetic field in opposite directions and with the analyser at an angle of 45^{o}. These demonstrate the saturated Faraday rotation.

Hänsch has recently reported[11] Doppler free polarization spectroscopy for the case of zero magnetic field. The present case can be analysed using similar techniques. The resulting intensity at the detector surface with the analyser at an angle θ is

$$I = \frac{I_o}{2}\left[(1 + \text{Cos } 2\,\theta) + \left(\frac{A}{1+X_+^2} + \frac{A}{1+X_-^2} + \frac{B}{1+X_o^2}\right)(1 + \text{Cos } 2\,\theta) + C\left(\frac{X+}{1+X_+^2} - \frac{X-}{1+X_-^2}\right)\text{sin } 2\,\theta\right] \qquad (1)$$

where I_o is the transmitted intensity without saturation. The paramter $X_{\pm} = (\nu-\nu_{\pm})/\Delta\nu_{\frac{1}{2}}$, where ν_0 is the center frequency of the unshifted transition, $\nu_{\pm}$ are the center frequencies of the shifted $\pm\sigma$ components,

and $\Delta\nu_{\frac{1}{2}}$ is the saturation line width. Thus $\frac{1}{1 + x^2}$ gives the saturated absorption line contours of the second term in (1) and $\frac{x}{1 + x^2}$ gives the saturated dispersion contours of the third term. When the analyser is parallel to the input polarization only the saturated absorption signal is observed, when perpendicular the intensity is zero, and for other angles both absorption and dispersion are observed. As discussed by Hänsch,[11] for $\theta = \pi/2$ the derivative with respect to θ of the dispersion term exceeds that of the absorption term.

The constants A, B and C determine the relative intensities of the saturated absorption $\pm\sigma$ peaks, the saturated absorption level crossing peak, and the saturated dispersion $\pm\sigma$ peaks, respectively. The ratio A:B was determined from the central ($\theta = 0$) curve of Fig. 6. Then C was found from the intensity needed to fit (1) to the curves for $\theta = 45^{o}$. The ratios A:B:C were determined in this way to be 2/3:1:2. In Fig. 7 an example of a fit using these ratios is shown for $\theta = 45^{o}$. The lower curve is the second term of (1); the central solid curve is the third term, the difference of the dashed + and - saturated dispersion curves; the upper solid curve is the total saturated Faraday rotation signal and is supperimposed on the dotted experimental curve. The discrepancy at the low intensity portions of the curve is caused by a small asymmetry in the $\pm\sigma$ components, corresponding to the measured tapering off of the solenoidal magnetic field toward the ends of the absorption cell.

Since saturated Faraday rotation is about 1000 times sharper than the linear effect, it may be of benefit in areas where the Faraday effect has been used such as the analysis of complex spectra.[12,13]

Ca Atomic Beam

In order to achieve the highest possible accuracy, we are using atomic beam techniques. Here one has the advantage of obtaining "isolated" atoms undergoing essentially no collisions with a relatively simple apparatus. Also, the optical excitation volume is small and hence can be easily shielded from extraneous electric and magnetic fields. The saturation signal can be obtained by measuring the beam intensity for one of the states of the transition. With a high efficiency beam detector, a large fraction of the optical transitions can be detected with the relatively small background of the quiet atomic beam, resulting in a very large S/N ratio close to the shot noise limit. This is in contrast to the low S/N which would be obtained with the usual technique of measuring the absorption in the optical signal. A sharp saturation peak with a width approaching the limit imposed by the radiative lifetime can be obtained by using a long atomic beam-laser beam interaction region.

A diagram of the atomic beam arrangement is shown in Fig. 8. The beam of ^1S_o ground state calcium atoms is produced by a resistively heated oven, collimated to have a Doppler width of 150 kHz, passed through the optical excitation region and deflecting magnet, and then is detected with a "single crystal" tungsten hot wire. The laser beam is directed perpendicularly across the atomic beam and then retroreflected with a cat's eye. The ground state atoms are not deflected by the magnet. When the laser frequency lies within the Doppler beam width, the atoms are excited to the paramagnetic $^3P_1$ state and then deflected, resulting in a signal decrease with the hot wire on axis (we have detected flop-out signals as high as 30% of the total beam). The saturation peak should appear as a sharp increased-intensity feature centered on the flop-out signal. Laser power of a few milliwatts is sufficient to give saturation.

Alternatively, the hot wire can be positioned off axis and the $^3P_1$ atoms deflected onto it. This provides the possibility of selecting a narrow slice of the axial velocity distribution; measurement of this velocity using first order Doppler techniques[14] should result in an accurate calculation of the second order Doppler shift correction.

In order to increase the optical interaction length, the approximately 2 mm diameter laser beam is expanded along the atomic beam axis with high quality cylindrical optics to a length of about 5 cm and is made plane to about $\lambda/3$ over this length. This should give a time-of-flight-limited saturated absorption linewidth of about 5 kHz, sufficient to completely resolve the recoil splitting of 23 kHz.

To date, we have not observed the saturation peak with the atomic beam due to poor magnetic shielding of the excitation region. The fringing field from the deflecting magnet has Zeeman broadened the line by a few hundred kHz so that we have observed only the broadened atomic beam width peaks such as that in Fig. 9, which has a linewidth (HWHM) of about 250 kHz. The prominent background fluctuations are due to changes in vacuum chamber pressure and have now been eliminated. A high quality magnetic shield is now being constructed which should lead to observation of the saturation peak. The low second order Zeeman shift for this transition, about 10^8 Hz/Tesla^2 (1 Hz/G^2), suggests the alternative technique of producing a small magnetic field at the interaction region, exciting only the $\Delta m = 0$ component, and then causing a Majarana flop in front of the deflecting magnet.

The saturation peak height should be about 50% of the flop-out signal and thus should have about the same S/N ratio. The flop-out signals we now observe have a S/N of 10^3 - 10^4 for one second integration. Thus for a 5 kHz wide line a setting precision $\Delta\nu/\nu$ of 10^{-14} - 10^{-15} in one second should be obtained. At this level, systematic offsets due to second order Doppler shift and laser beam wavefront curvature must be considered.

As mentioned above, the velocity of the atoms being observed, and hence the second order Doppler shift, can be measured using first order Doppler techniques as discussed by Bergmann et al[14]. With these techniques it should be possible to reduce the second order shift to below 10^{-15}.

The problem of wavefront curvature is more difficult to solve. Use of a plane-parallel cavity for the excitation region reduces the curvature; even with this technique it is doubtful that the offset could be reduced much below 1 X 10^{-14} when the laser beam is perpendicular to the atomic beam. However, it is possible to obtain the saturation peak with the laser beam intersecting the atomic beam at a small angle by having the forward and return laser beams symetrically offset in frequency from line center.[15] This reduces the wavefront curvature shift by the sin of the angle.[16] By having an intersecting angle of only a few degrees this offset should be greatly reduced. Since for this condition only atoms from a narrow slice of the Boltzman axial velocity distribution are observed, the saturation peak height will be reduced requiring a longer integration time to recover S/N. With a compromise between reduction of shift and loss of S/N a frequency reproducibility close to 10^{-15} may be achieved.

Summary

The high level of stability now obtained with cw dye lasers is leading to consideration of new candidates for wavelength/frequency standards in the visible. The investigations with calcium discussed above indicate two possible approaches. First, use of a simple absorption cell to obtain an excellent intermediate accuracy standard; this should have an accuracy much higher than that of the iodine-stabilized He-Ne laser. Second, use of an atomic beam to obtain a standard with the highest possible accuracy. This promises to give an accuracy of about 10^{-15}, making the ^1S_o-$^3P_1$ transition in calcium one of the best candidates for an ultra-high accuracy standard in the visible.

TABLE I

PROPERTIES OF THE CALCIUM $^1S_0$ - $^3P_1$ TRANSITION AS A POSSIBLE FREQUENCY/WAVELENGTH STANDARD IN THE VISIBLE

Bohr frequency	(λ_{vac} = 6574.593 0 Å)
Lifetime of $^3P_1$	0.39 ms
Ultimate natural linewidth (FWHM)	410 Hz
Lifetime - limited Q	1×10^{12}
Recoil splitting	23 kHz
First - order Doppler	none (saturation spectroscopy)
Second - order Doppler	-1.7 #kHz $\left[-5 \times 10^{-15}/°C\right]$
Zeeman effect	$\sim 10^8$ Hz/Tesla^2 (1 Hz/G^2) $\left[2 \times 10^{-15}/G^2\right]$
Stark effect	$\lesssim$1 Hz/(V/cm)^2 $\left[2 \times 10^{-15}/(V/cm)^2\right]$
Optimum laser power	$\simeq$5 mW
Intensity dependent	none (recoil doublet resolved)

References

1. R. L. Barger, J. B. West and T. C. English, Appl. Phys. Lett. 27 31 (1975).
2. R. L. Barger, T. C. English and J. B. West, Proceedings of the Twenty-Ninth Annual Frequency Control Symposium 1975, P. 316 (Electronic Industries Assoc., 2001 Eye St. N.W., Washington, D.C. 20006).
3. Strumia has suggested use of a fine structure transition of the ^3P state as a frequency standard. F. Strumia, Metrologia 8, 85 (1972).
4. P. L. Bender, J. L. Hall, R. H. Garstang, F. M. J. Pichanick, W. W. Smith, R. L. Barger, and J. B. West, Bull. Am. Phys. Soc. Series II, Vol. 21, No. 4, pp 599 (1976).
5. The fast amplifier used for the intensity stabilization, and the similar one used for frequency stabilization, were designed by J. L. Hall. A slow version of a similar intensity stabilizer is described in W. Hartig and H. Walther, Appl. Phys. 1, 171 (1973).
6. P. S. Furcinitti, L. C. Balling and J. J. Wright, Phys. Lett. 53A, 75 (1975).
7. J. J. Snyder, Appl. Opt. 14, 1825 (1975).
8. M. Faraday, Phil. Trans. 3, 1 (1846).
9. R. W. Wood, Physical Optics, 3rd ed. (pp 709), Dover Publication, Inc. New York.
10. The presence of the Doppler-generated level crossing peak in Zeeman spectra is discussed in E. E. Uzgiris, J. L. Hall and R. L. Barger, Phys. Rev. Lett. 26, 289 (1971).
11. C. Wieman and T. W. Hänsch, Phys. Rev. Lett. 36, 1170 (1976).
12. P. Kusch and M. M. Hessel, J. Mol. Spectr. 32, 181 (1969).

13. See, for instance, Magneto Optical Effects, Symposia of the Faraday Society No. 3 (1969), The Aberdeen University Press Ltd, Aberdeen, Scotland.

14. K. Bergmann, W. Demtröder and P. Hering, Appl. Phys. 8, 65 (1975).

15. Two-frequency saturation has been observed for the 3.39 μm line of CH_4 by R. L. Barger and J. L. Hall (unpublished).

16. J. L. Hall in Proceedings of the URSI General Assembly, Lima, Peru, (1975), and J. L. Hall, Opt. Comm. 18 (1976).

Figure Captions

1. Dye laser stabilization scheme.
2. Allan variance (σ) vrs. integration time (τ) for stabilized dye laser.
3. Diagram of calcium absorption cell showing polarization scheme for detection of saturated Faraday rotation.
4. Ca ^1S_o-$^3P_1$ saturation peak obtained with absorption cell. HWHM is about 2 MHz.
5. Early observations of Doppler width Faraday rotation in sodium. Reproduced from R. W. Wood's Physical Optics, with permission of the publishers.
6. Saturated Faraday rotation in the ^1S_o-$^3P_1$ line of calcium. Upper and lower curves with analyser at 45^o and magnetic field in opposite directions; center curve with analyser at 0^o shows only saturated absorption Zeeman pattern.
7. Fit of theory to experiment for $\theta = 45^o$. Experimental data is dotted trace of upper curve.
8. Diagram of atomic beam apparatus.
9. Ca beam on-axis signal. HWHM $\simeq$ 250 kHz. Background fluctuations are due to changes in vacuum chamber pressure and have now been eliminated.

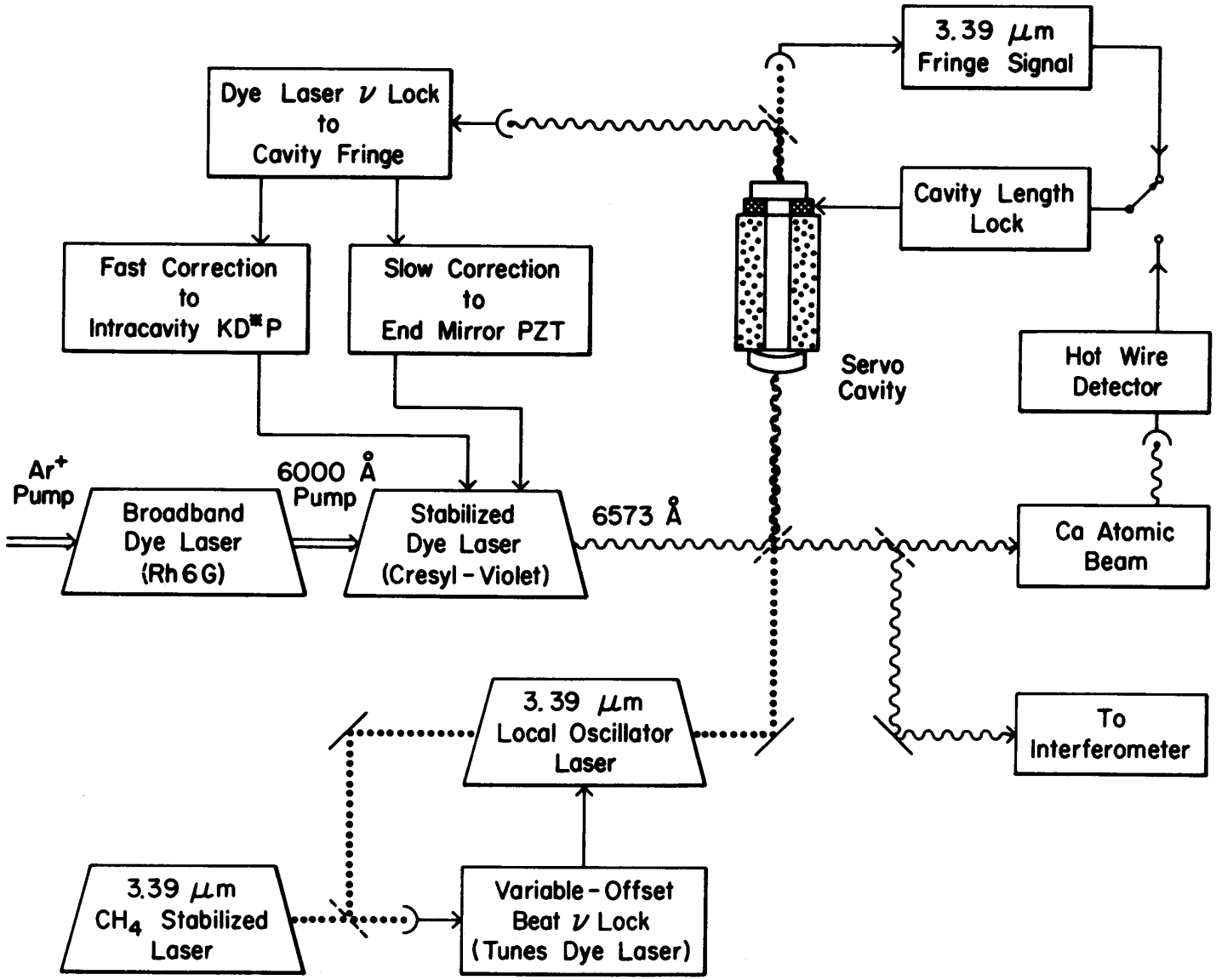

FIGURE 1

76X0464

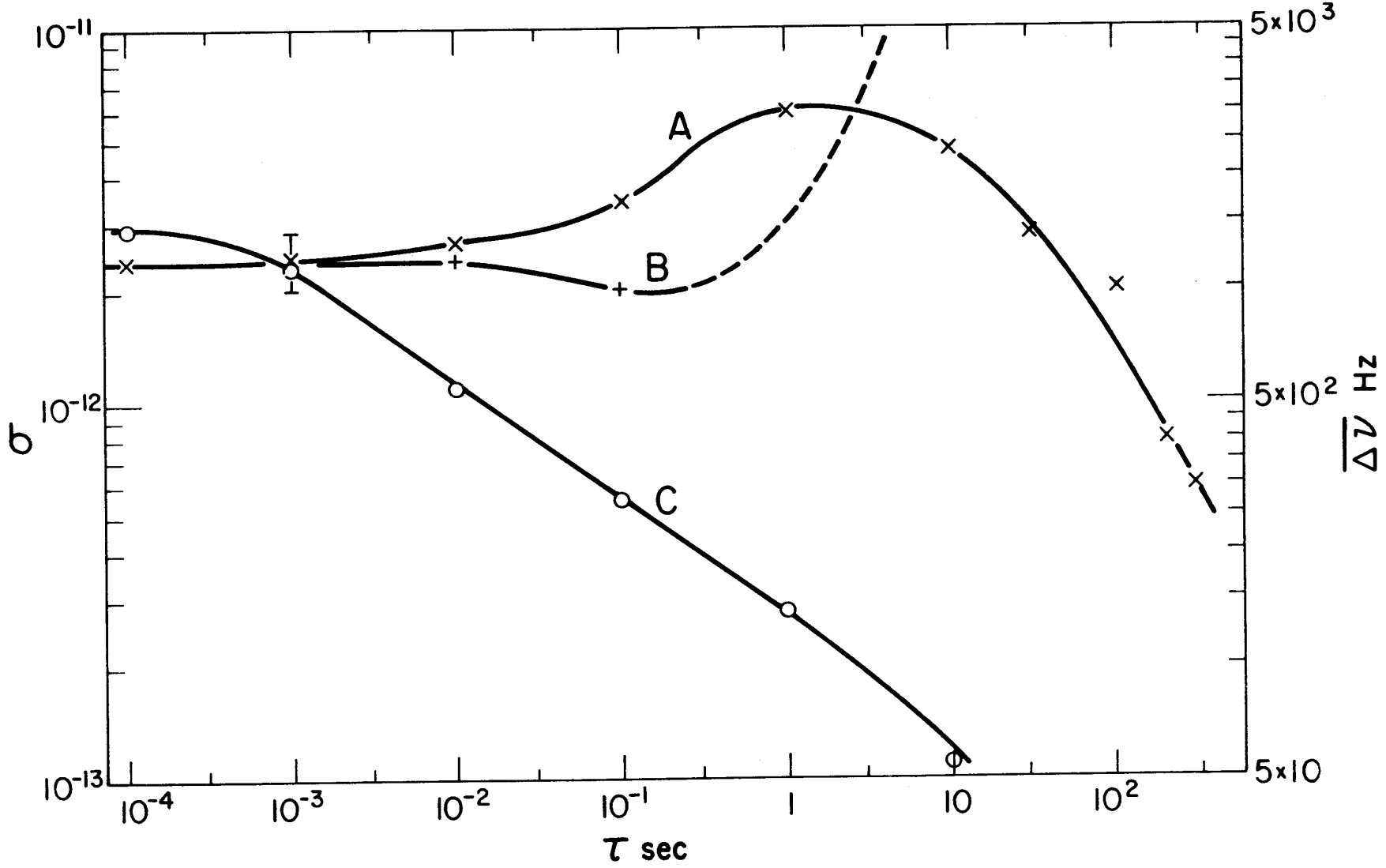

FIGURE 2

75x 4560

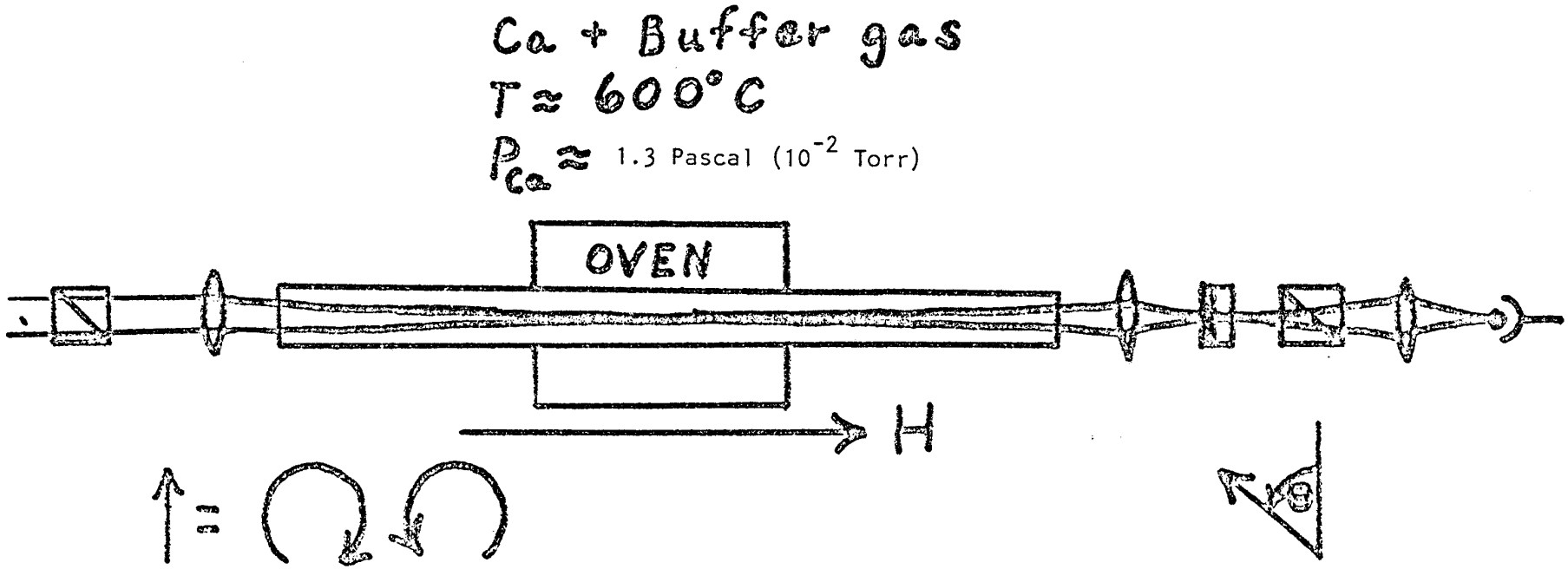

FIGURE 3

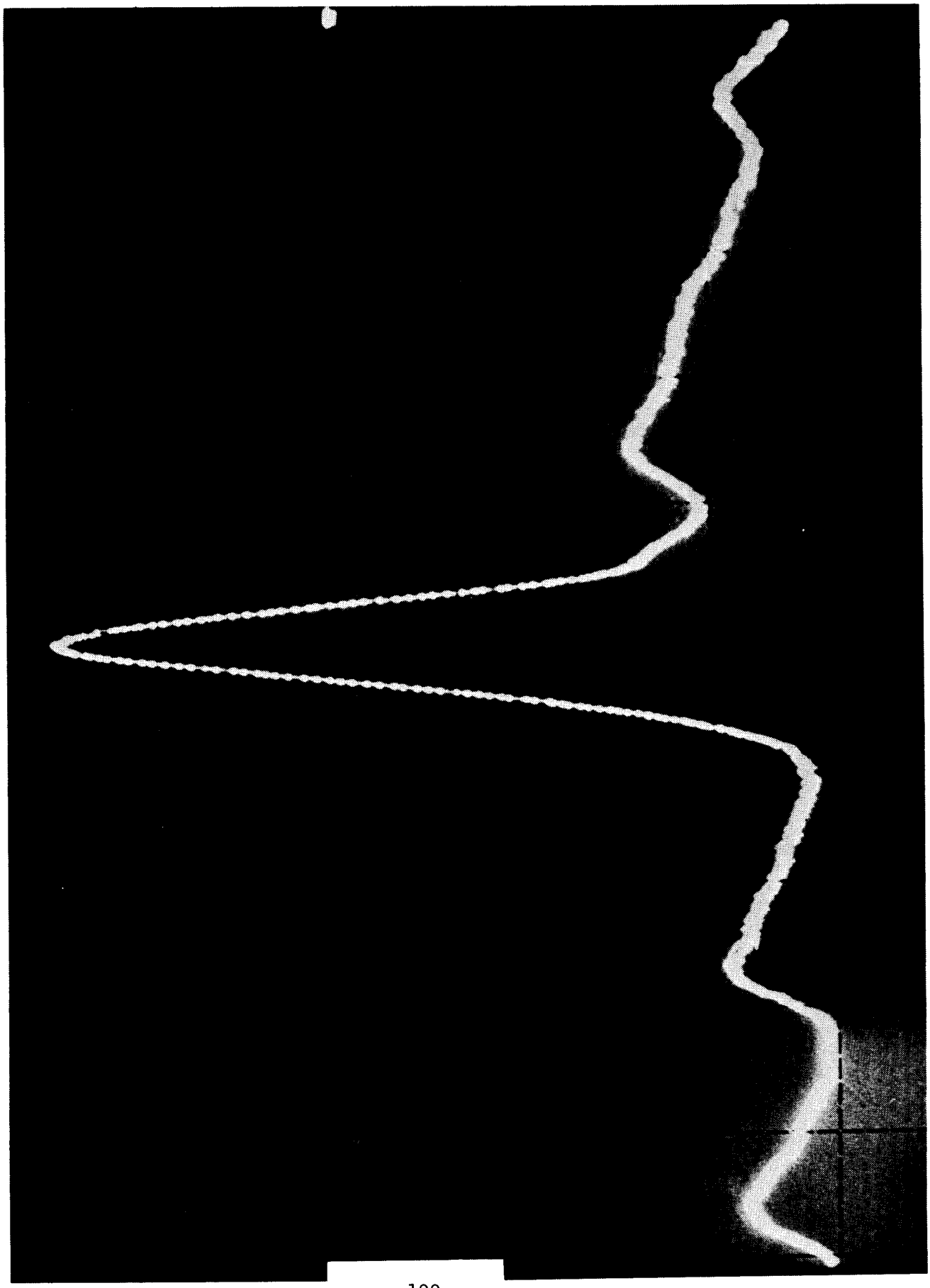

FIGURE 4

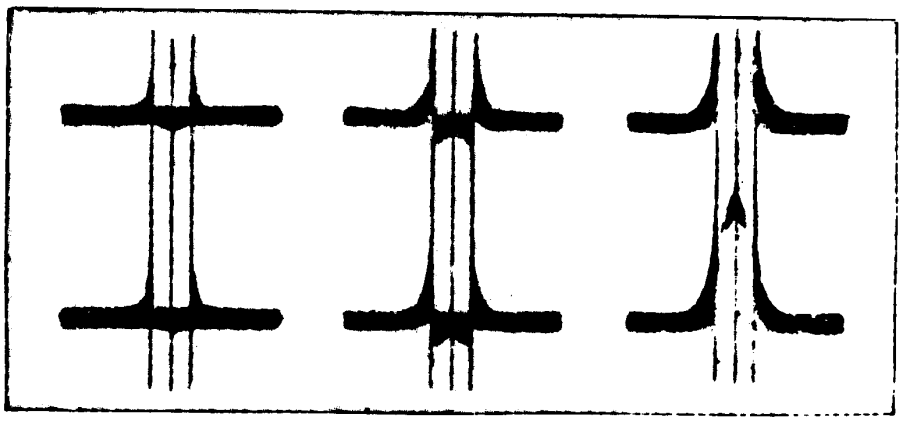

FIG. 400

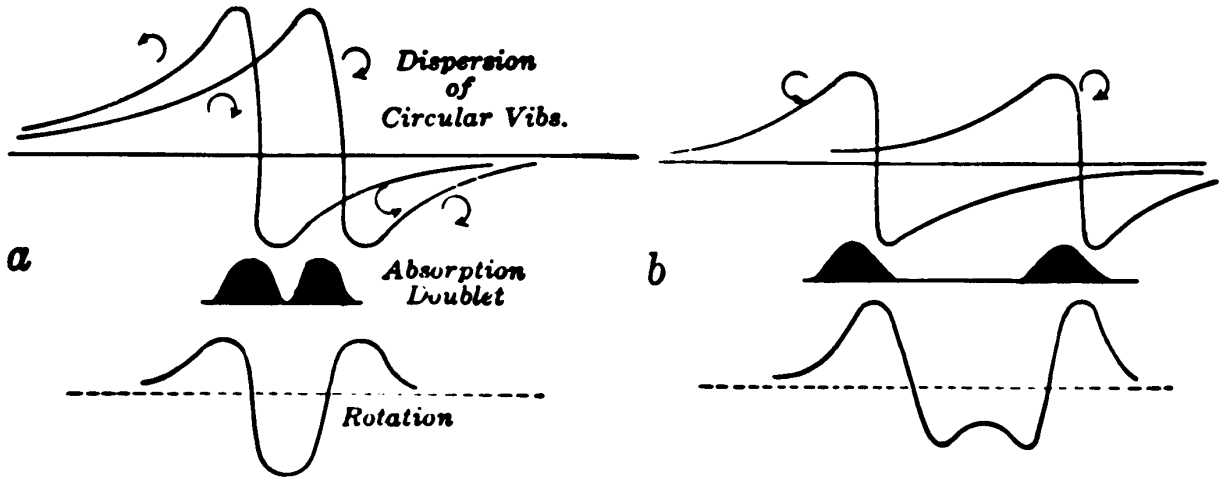

FIG. 403

From Physical Optics, R. W. Wood

Reproduced By Permission of Dover Publications, Inc., New York.

FIGURE 5

77X 0007

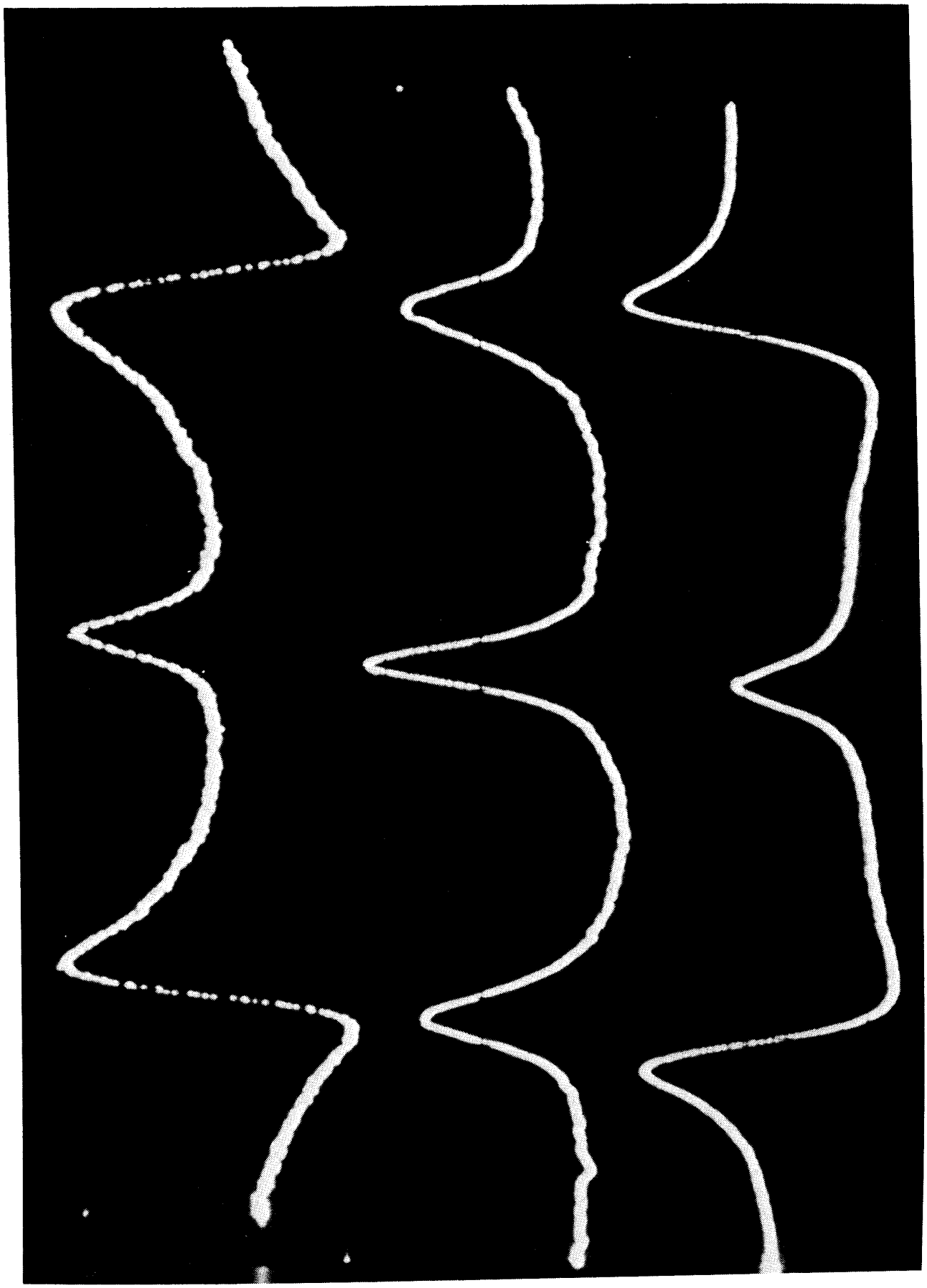

FIGURE 6

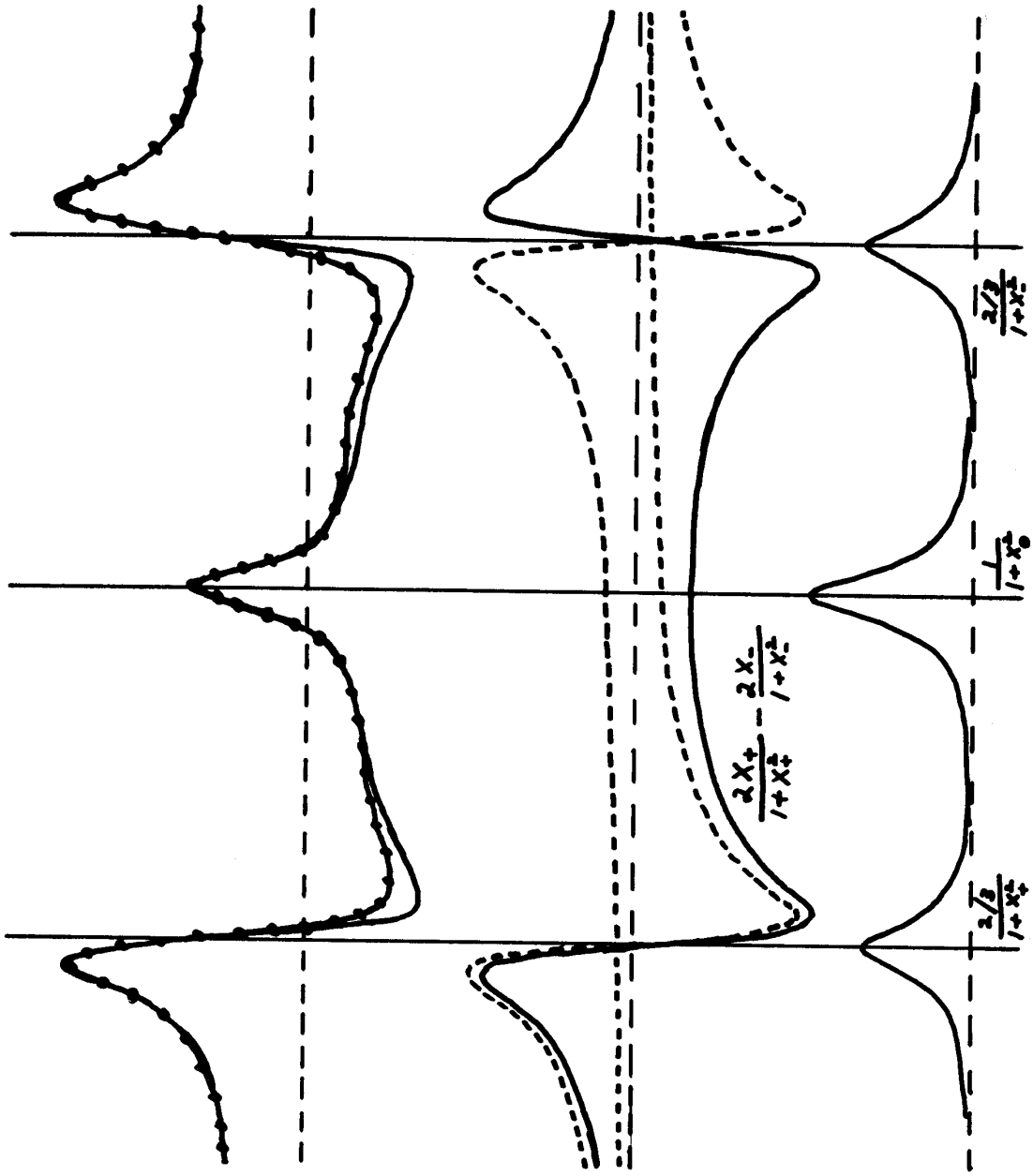

FIGURE 7

77X 0006

SATURATION SPECTROSCOPY OF CALCIUM

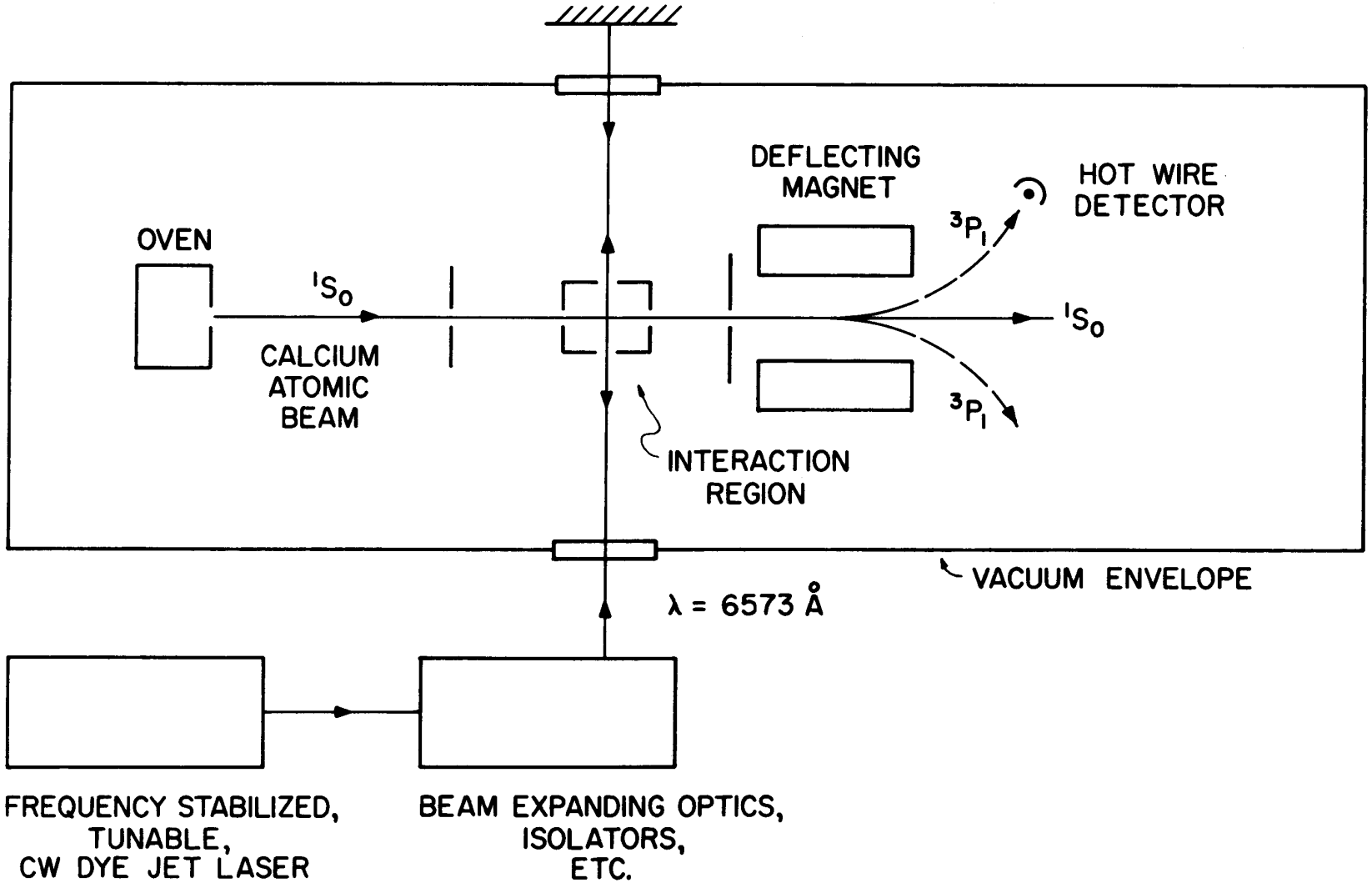

FIGURE 8

76X0463

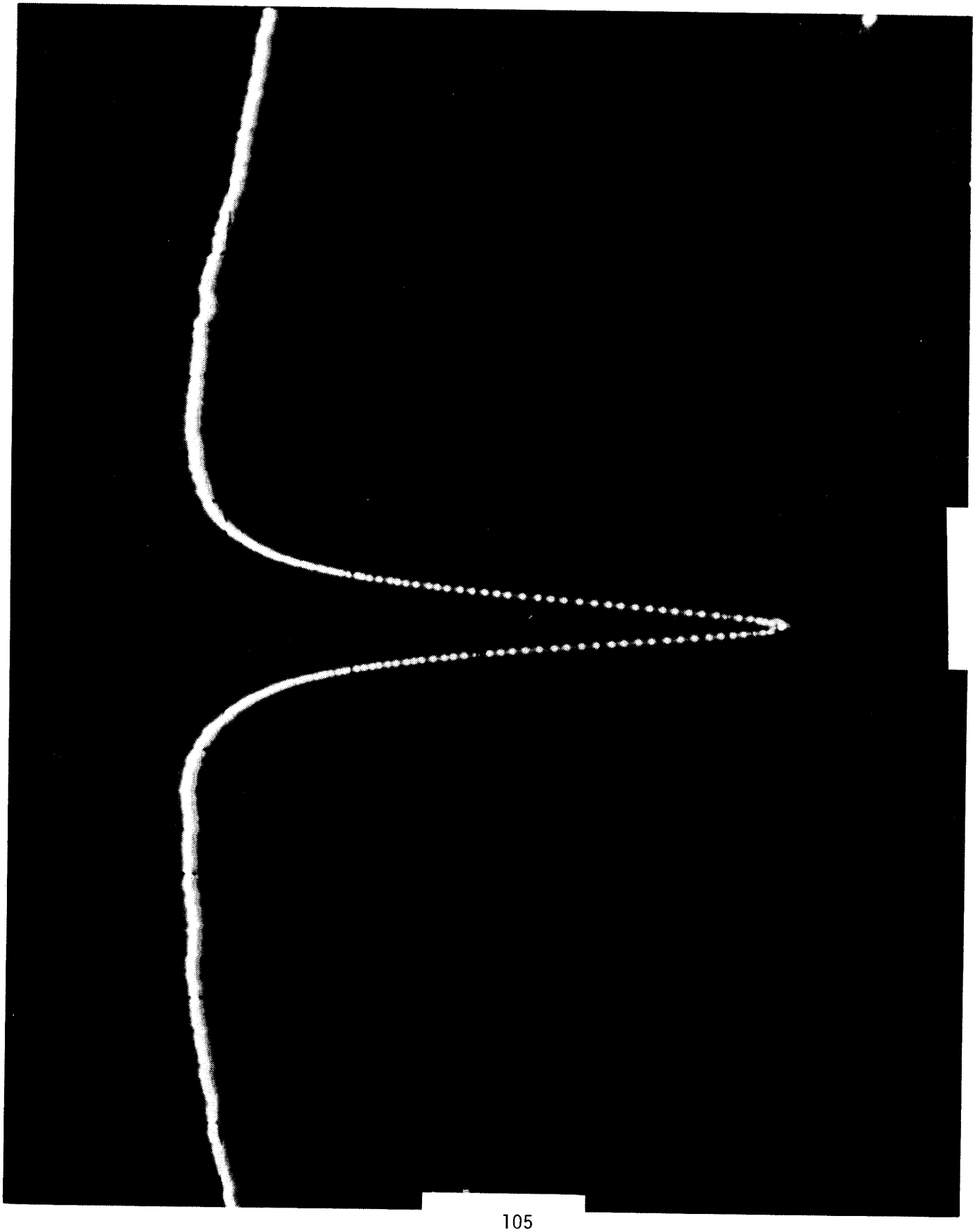

FIGURE 9

TABLE I

PROPERTIES OF THE CALCIUM $^1S_0$ - $^3P_1$ TRANSITION AS A POSSIBLE FREQUENCY/WAVELENGTH STANDARD IN THE VISIBLE

Bohr frequency	(λ_{vac} = 6574.593 0 Å)
Lifetime of $^3P_1$	0.39 ms
Ultimate natural linewidth (FWHM)	410 Hz
Lifetime - limited Q	1×10^{12}
Recoil splitting	23 kHz
First - order Doppler	none (saturation spectroscopy)
Second - order Doppler	-1.7 #kHz $\left[-5 \times 10^{-15}/^{o}C\right]$
Zeeman effect	~1 Hz/G^2 $\left[2 \times 10^{-15}/G^2\right]$
Stark effect	$\lesssim$1 Hz/(V/cm)^2 $\left[2 \times 10^{-15}/(V/cm)^2\right]$
Optimum laser power	~5 mW
Intensity dependent	none (recoil doublet resolved)

77X 0009